Structure-Preserved Power System Transient Stability Using Stochastic Energy Functions

Theresa Odun-Ayo, *Student Member, IEEE*, and Mariesa L. Crow, *Fellow, IEEE*

***Abstract*—With the increasing penetration of renewable energy systems such as plug-in hybrid electric vehicles, wind and solar power into the power grid, the stochastic disturbances resulting from changes in operational scenarios, uncertainties in schedules, new demands and other mitigating factors become crucial in power system stability studies. This paper presents a new method for analyzing stochastic transient stability using the structure-preserving transient energy function. A method to integrate the transient energy function and recloser probability distribution functions is presented to provide a quantitative measure of probability of stability. The impact of geographical distribution and signal-to-noise ratio on stability is also presented.**

***Index Terms*—Energy functions, stochastic differential algebraic equations, structure-preserved power system, transient stability.**

I. Introduction

ELECTRICAL power system loads are functions of a myriad of active and reactive power demands that depend on a variety of factors including time, weather, geography, and economics. The result of the aggregate behavior of many thousands of individual customer devices switching independently are power system loads that are stochastic in nature. The variability of the electrical network loading has received increased attention in recent years due to the expansion of renewable resources and the likelihood of wide-spread adoption of plug-in electric vehicles (PEVs) [1]. Renewable energy resources such as wind turbines or solar power can introduce uncertainty into the power system as a result of atmospheric variations causing excursions in active power generation. Furthermore, plug-in electric vehicles are a potential significant source of disturbance on the grid due to their battery charge and discharge characteristics. The tandem effect of renewable resources and PEVs may create uncertainties of such significant magnitude they impact the operation of the power system.

The study and analysis of stochastic power system dynamics is not a new topic; it has been studied for several decades [2]–[5], but has received renewed interest in recent years as the amount of uncertainty in the system has increased [6]–[9]. The inclusion of stochasticity in power systems may lead to very different stability results from a deterministic approach. For example, even though a deterministic power system might be stable, small random perturbations may cause the state trajectories to reach a critical point such that exceeding this point may cause the system to collapse or enter an undesirable operating state [10]. As power system loads and generation become increasingly non-deterministic, it is essential that analytical methods be developed to analyze the behavior of the stochastic system to better understand the inherent risks and provide sufficient protection against failures.

Power system transient stability is typically assessed either through direct methods (such as Lyapunov-based energy functions), or through time-domain simulation [11]–[15]. The inclusion of randomness into transient stability analysis most often requires the use of Monte Carlo methods to ascertain the behavior of the system over multiple trials. The basic idea for a Monte Carlo approach to transient stability assessment using transient energy functions was first proposed in [4], but the appropriate stochastic tools did not exist at that time to frame the stochastic energy function nor to numerically solve the stochastic differential equations.

Since the stochastic behavior of the power system is typically manifested through the variance of the loads, the choices of power system model and the particular transient stability assessment method are crucial. In many Lyapunov-based transient stability studies, the system energy function is developed for the "classical model" in which the load impedance is absorbed into an equivalent reduced network as viewed from the generator buses. In such a scheme, the structure of the original network is lost. Although the classical model is frequently used in transient stability direct methods, this model is known to have several shortcomings: 1) it precludes the consideration of reactive power demand and voltage variation at the load buses; and 2) the reduction of the impedance network leads to a loss of system topology and hence precludes the study of how the transient energy varies among different components of the network [12]–[15]. An alternative approach is to adopt the structure preserving model in which the active and reactive demand at each load bus is explicitly represented. The use of a structure preserving model of the system, first proposed by Bergen and Hill [16], aims at overcoming some of the shortcomings of the classical model, thereby allowing accurate modeling of loads. The structure preserved model maintains the original network and uses the unreduced admittance matrix, resulting in a model that can be regarded as having structural integrity [17].

Since the time of [4], there has been considerable progress made in the development of the appropriate tools necessary to address stochastic transient stability. There have been numerous recent advances in the application of Lyapunov stability methods to stochastic differential equation systems [19]–[21].

Manuscript received July 12, 2011; revised November 09, 2011; accepted December 22, 2011. Date of publication February 15, 2012; date of current version July 18, 2012. This work was supported in part by a grant from the National Science Foundation under EFRI-080322. Paper no. TPWRS-00657-2011.

The authors are with the Electrical and Computer Engineering Department, Missouri University of Science and Technology, Rolla, MO 65409-0810 USA (e-mail: taohy8@mst.edu; crow@mst.edu).

Digital Object Identifier 10.1109/TPWRS.2012.2183396

Furthermore, the past decade has seen significant advances in the development of numerical integration methods to simulate stochastic (ordinary) differential equations [22]. *In this paper, these advances in stochastic Lyapunov stability methods and the numerical solution of systems of stochastic differential equations will be merged to present a novel approach to developing a quantitative measure of probability of stability that is suitable for power system risk assessment.*

II. Structured Preserved Stochastic Transient Energy Functions

The concept of transient stability is based on whether, for a given disturbance, the trajectories of the system states during the disturbance remain in the domain of attraction of the post-disturbance equilibrium when the disturbance is removed. Transient instability in a power system is caused by a severe disturbance which creates a substantial imbalance between the input power supplied to the synchronous generators and their electrical outputs. Some of the severely disturbed generators may "swing" far enough from their equilibrium positions to lose synchronism. Such a severe disturbance may be due to a sudden and large change in load, generation, or network configuration. Since large disturbances may lead to nonlinear behavior, Lyapunov functions are well-suited to determine power system transient stability. Since true Lyapunov functions do not exist for lossy power systems, so-called "transient energy functions" are frequently used to assess the dynamic behavior of the system [25]. From a modeling point of view, the structure preserved model allows a more realistic representation of power system components including load behaviors and generator dynamic models.

To better understand how the structure preserved transient energy function will be developed and analyzed, a brief review of Lyapunov functions for stochastic differential equations is first presented.

Consider the nonlinear stochastic system

$$dx = f(x,t)dt + g(x,t)\Sigma(t)dW(t) \quad x(0) = x_0 \in \mathbb{R}^n \tag{1}$$

whose solution can be written in the sense of Ito:

$$x(t) = x_0 + \int_0^t f(x,s)ds + \int_0^t g(x,s)\Sigma(s)dW(s) \tag{2}$$

where $x(t) \in \mathbb{R}^n$ is the state; $W(t)$ is an m-dimensional standard Wiener process defined on the complete probability space $(\Omega, \mathcal{F}, P)$; the functions (f, g) are locally bounded and locally Lipschitz continuous in $x \in \mathbb{R}^n$ with $f(0,t) = 0$, $g(0,t) = 0$ for all $t \geq 0$; and the matrix $\Sigma(t)$ is nonnegative-definite for each $t \geq 0$. These conditions ensure uniqueness and local existence of strong solutions to (1) [19], [26].

As with many nonlinear deterministic systems, Lyapunov functions can provide guidance regarding the stability of stochastic differential equation (SDE) systems. An SDE system is said to satisfy a stochastic Lyapunov condition at the origin if there exists a proper Lyapunov function $V(x)$ defined in a neighborhood D of the origin in $\mathbb{R}^n$ such that

$$\mathcal{L}V(x) \leq 0 \tag{3}$$

for any $x \in D\backslash\{0\}$ where the differential generator $\mathcal{L}$ is given by

$$\mathcal{L}V(x,t) = \frac{\partial V}{\partial x} f(x,t) + \frac{1}{2}\mathrm{Tr}\left\{\Sigma(t)^T g(x,t)^T \frac{\partial^2 V}{\partial x^2} g(x,t)\Sigma(t)\right\}. \tag{4}$$

If (3) is satisfied, then the equilibrium solution $x(t) \equiv 0$ of the stochastic differential (1) is considered to be *stable in probability* [27].

To accurately include the effects of the loads in the system, the so-called structure-preserved, center-of-intertia model of the power system is used, such that [16], [18]

$$\dot{\theta}_i = \tilde{\omega}_i \tag{5}$$

$$M_i\dot{\tilde{\omega}}_i = P_{M_i} - \sum_{j=1}^{n} B_{ij}V_iV_j\sin(\theta_i - \theta_j) - \frac{M_i}{M_T}P_{COI} \quad i = 1,\ldots,m \tag{6}$$

$$0 = P_{d_i}^0 + D_i\dot{\theta}_i + \sum_{j=1}^{n} B_{ij}V_iV_j\sin(\theta_i - \theta_j) \tag{7}$$

$$0 = Q_{d_i} + \sum_{j=1}^{n} B_{ij}V_iV_j\cos(\theta_i - \theta_j) \quad i = m+1,\ldots,n \tag{8}$$

where

$$\theta_i = \delta_i - \delta_0$$
$$\tilde{\omega}_i = \omega_i - \omega_0$$

and

$$\delta_0 = \frac{1}{M_T}\sum_{i=1}^{m} M_i\delta_i; \quad \omega_0 = \frac{1}{M_T}\sum_{i=1}^{m} M_i\omega_i;$$
$$M_T = \sum_{i=1}^{m} M_i$$
$$P_{COI} = \sum_{i=1}^{m}\left(P_{M_i} - \sum_{j=1}^{n} B_{ij}V_iV_j\sin(\theta_i - \theta_j)\right) \tag{9}$$

where

δ_i	generator rotor angle;
θ_i	COI bus angle;
ω_i	generator angular frequency;
$\tilde{\omega}_i$	COI angular frequency;
M_i	inertia constant;
P_{M_i}	mechanical output;
V_i	bus voltage;
B_{ij}	(i,j)th entry of the reduced lossless admittance matrix;
D_i	positive sensitivity coefficient representing the load frequency dependence;
m	number of generators in the system;
n	number of total buses in the system;
ω_s	synchronous speed in radians

and P_{d_i} and Q_{d_i} are the load demands at each bus i in the system.

The corresponding energy function is [18]

$$\begin{aligned} &V\left(\tilde{\omega}_{gi},\theta,V\right) \\ &= \frac{1}{2}\sum_{i=1}^{m} M_i\tilde{\omega}_{gi}^2 - \sum_{i=1}^{m} P_{M_i}\left(\theta_i-\theta_i^s\right) + \sum_{i=1}^{n+m} P_{d_i}\left(\theta_i-\theta_i^s\right) \\ &- \frac{1}{2}\sum_{i=1}^{n+m} B_{ii}\left(V_i^2-\left(V_i^s\right)^2\right) + \sum_{i=1}^{n+m}\frac{Q_{d_i}^s}{a\left(V_i^s\right)^a}\left(V_i^a-\left(V_i^s\right)^a\right) \\ &- \sum_{i=1}^{n+m-1}\sum_{j=i+1}^{n+m} B_{ij}\left(V_iV_j\cos(\theta_i-\theta_j)-V_i^sV_j^s\cos(\theta_i^s-\theta_j^s)\right) \end{aligned} \tag{10}$$

where a is usually 2 and the superscript "s" indicates the stable equilibrium point. It is assumed that the power system frequency deviations (see [28] for a recent example) can be represented by an appropriately scaled Wiener process $W_i(t)$ (i.e., zero mean, finite covariance). Note that this is why the load variation is represented by a Wiener process as opposed to a Gaussian noise input $(dW_i(t))$. Therefore a frequency dependent load gives rise to

$$P_{d_i} = P_{d_i}^0 + D_i\dot{\theta}_i \tag{11}$$
$$= P_{d_i}^0 + D_i\left(\omega_i-\omega_s\right) \tag{12}$$
$$= P_{d_i}^0 + D_iW_i(t) \tag{13}$$
$$= P_{d_i}^0\left(1+\alpha_{P_i}W_i(t)\right) \tag{14}$$

where $\alpha_{P_i} = D_i/P_{d_i}^0$. Similarly (but less commonly)

$$Q_{d_i} = Q_{d_i}^0\left(1+\alpha_{Qi}W_i(t)\right) \tag{15}$$

where P_{di}^0, Q_{di}^0 are the mean values of the active and reactive load at bus i, respectively, and α_{Pi}, α_{Qi} are the magnitudes of the active and reactive noise. Note that the variance in the noise (i.e., standard deviation) is not explicitly represented but is inherent in the construction of the Weiner process $W_i(t)$. The magnitude of the scaling coefficients α_{P_i}, α_{Q_i} depends on the level of penetration of low-inertia renewable resources (wind turbines, photovoltaics) and loads (such as electric vehicles). The full set of SDAEs for the power system are given by

$$\dot{\theta}_i = \tilde{\omega}_i \tag{16}$$

$$M_i\dot{\tilde{\omega}}_i = P_{M_i} - \sum_{j=1}^{n} B_{ij}V_iV_j\sin\left(\theta_i-\theta_j\right) - \frac{M_i}{M_T}P_{COI} \qquad i=1,\ldots,m \tag{17}$$

$$0 = P_{d_i}^0\left(1+\alpha_{P_i}W_i(t)\right) + \sum_{j=1}^{n} B_{ij}V_iV_j\sin(\theta_i-\theta_j) \tag{18}$$

$$0 = Q_{d_i}^0\left(1+\alpha_{Qi}W_i(t)\right) + \sum_{j=1}^{n} B_{ij}V_iV_j\cos(\theta_i-\theta_j) \qquad i=m+1,\ldots,n. \tag{19}$$

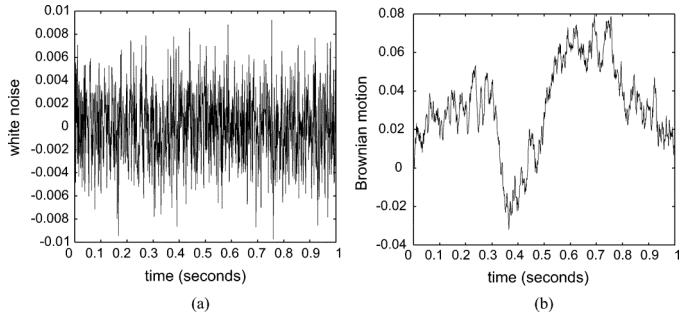

Fig. 1. (a) Load Gaussian noise and (b) resulting Brownian motion.

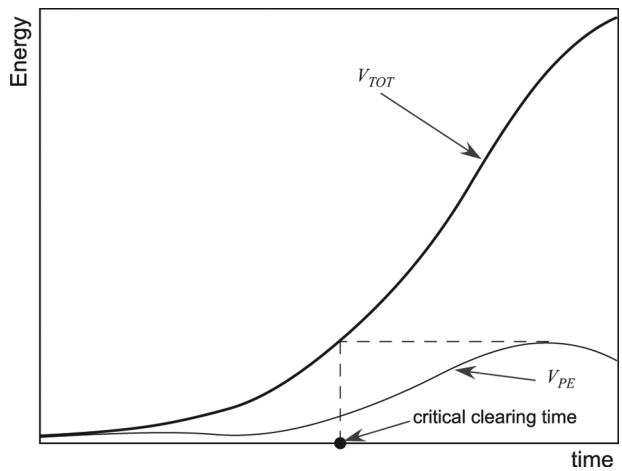

Fig. 2. Total energy V_{TOT} versus the potential energy V_{PE}. The critical clearing time is the time at which the total energy equals the maximum potential energy.

Similar to the approach proposed in [10], the load and generation disturbances are modeled stochastically with varying magnitudes depending on bus location in the system. In this paper, we consider only the impact of Gaussian variation (normal distribution), but other distributions can be incorporated. For example, wind generation is often modeled as a Weibull distribution [23], whereas PHEV distributions have been suggested to be Poisson distribution [24]. The load power is assumed to vary stochastically with an expected value of the base case loading. The loads at each bus are modeled by a random walk (Brownian motion) derived from a Gaussian (white) random process [$dW(t)$ from (1)] as shown in Fig. 1(a). The resulting load variation takes the form shown in Fig. 1(b).

III. Methodology

The closest unstable equilibrium point (UEP) and controlling UEP method are two common direct methods used to assess the system's stability [25]. The controlling UEP method consists of numerically integrating the system state and calculating the kinetic, potential, and total energy of the fault-on system until the point at which the potential energy reaches its maximum value. The critical clearing time (CCT) of the system is then calculated by finding the time at which the total energy is equal to the maximum potential energy as shown in Fig. 2.

The total energy V_{TOT} is the sum of the potential energy V_{PE} and the kinetic energy V_{KE}. While it may appear as if there is

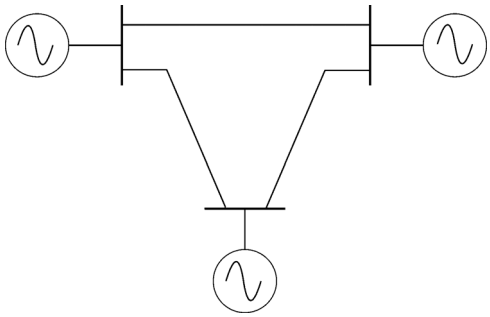

Fig. 3. Small test system.

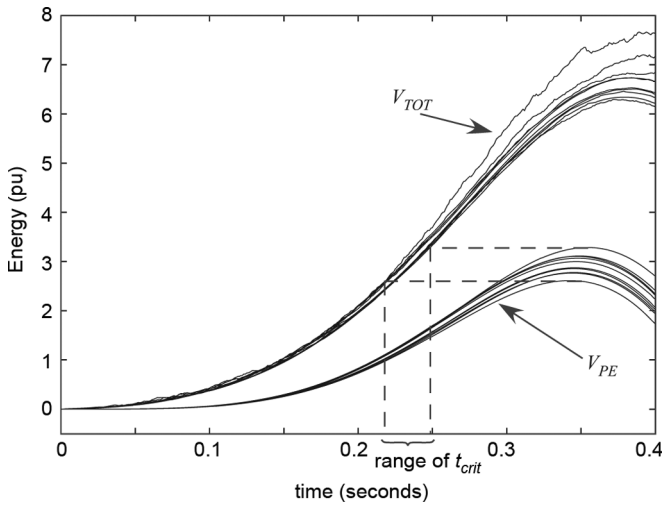

Fig. 4. Illustration of change in t_{crit} over the range of 10 runs—upper plots show the total energy V_{TOT}, lower plots show potential energy V_{PE}.

negligible impact of stochasticity on the potential energy, this is not the case. The kinetic energy term is dominated by the generator frequencies which are directly and significantly influenced by the random load perturbations; thus, the total energy directly reflects this variation. The potential energy term is dominated by the generator angles variations, which are the integral of the frequencies. This integral relationship tends to act as a filter for the load variations; thus, the potential energy term appears to be smoother than the total energy.

The energy function approach for determination of transient stability is applied to the system of stochastic differential-algebraic equations for a small three-bus test system (Fig. 3), and a Monte Carlo approach has been used to construct the probability distribution of the critical clearing time of the stochastic system. Ten consecutive simulations with the same Gaussian noise magnitude and variance but different noise sets yields the set of energies V_{TOT} and V_{PE} shown in Fig. 4.

These responses demonstrate that the stability of the power system may be significantly affected by injecting stochasticity into the loads. Fig. 5 shows a histogram of the critical clearing times obtained from 1000 transient stability runs. This histogram was generated by calculating the critical clearing time of 1000 runs of the energy function method. This set of critical clearing times ranges from a minimum of $t_{crit} = 0.2025$ s to a maximum of $t_{crit} = 0.2385$ s with a mean value of

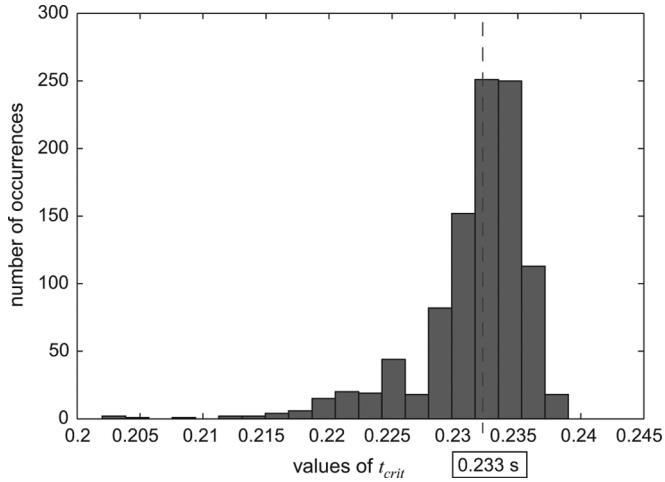

Fig. 5. Histogram of t_{crit} (1000 runs).

$t_{crit} = 0.233$ s. Note that the mean CCT value 0.233 s is also the same CCT obtained from a single deterministic run of the energy method. Note that if another 1000 runs were performed with different Gaussian noise sets (with the same standard deviation), this histogram would most likely look slightly different, but would have the same general distribution and would probably yield the same mean value. But in the cumulative effect as the number of runs becomes large, the mean results should approach the same response. Even though the mean value of the histogram (and the probability distribution function in the limit as the number of runs goes to infinity) is the same as the deterministic critical clearing time, this does not indicate that this is a redundant result. The probabilistic approach provides additional information regarding level of acceptable risk associated with the critical clearing time. For example, if a recloser were set to clear the fault at 0.225 s, this would be a fully sufficient setting in the deterministic analysis, since 0.225 s is less than the critical clearing time. However, in the probabilistic analysis, there is still a finite probability that the system would be unstable with a clearing time of 0.225 s. From the histogram in Fig. 5, the histogram indicates that the system will be stable for 958 runs/1000 runs or 96%. This metric provides a measure of risk associated with a particular clearing time.

For a large sample population, the histogram of critical clearing times predicts the shape of the probability density function. Of significant note is that for a standard deviation and variance of 1.0, the median value of the histogram is the same as the deterministic critical clearing time. This implies that half of the CCTs are greater than 0.233 s and half are smaller. Note however that even though the expected value is the same as the deterministic CCT, the variance is not symmetric about the median even though the load perturbations are Gaussian distributed.

One way to interpret these results is to combine the critical clearing time distribution with a recloser distribution. The probability of maintaining stability P_S is then given by

$$P_S = \int_{\tau_r=0}^{\tau_r=\infty} \int_{\tau_d=0}^{\tau_d=\tau_r} f_{CCT}(\tau_r)\, f_R(\tau_d)\, d\tau_r d\tau_d \qquad (20)$$

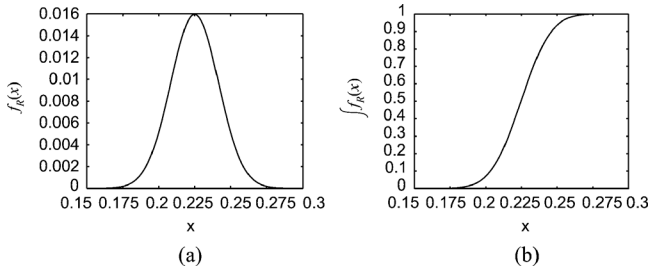

Fig. 6. Recloser distribution function with $\mu = 0.225$ s and $\sigma = 1/60$ s. (a) Probability distribution function. (b) Cumulative distribution function.

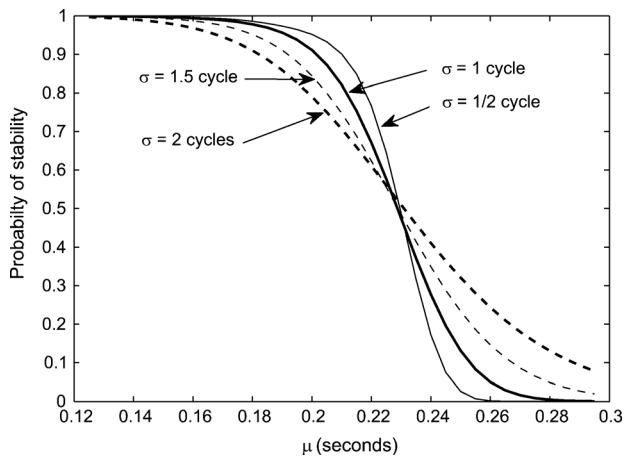

Fig. 7. Probability of stability as a function of recloser action expected value μ with varying σ.

where f_R is the probability distribution of the recloser and f_{CCT} is the probability distribution function of the critical clearing times [29].

For example, consider a recloser probability distribution function shown in Fig. 6. The recloser action is a Gaussian distribution with an actuation mean time of 0.225 s and a one cycle standard deviation. The probability distribution of the critical clearing times cannot be represented by a closed form distribution, but the P_S can be estimated by

$$P_S \approx \sum_{k_d=1}^{N} \sum_{k_r=1}^{k_d} \hat{f}_{CCT}(k_r)\, \hat{f}_R(k_d) \tag{21}$$

where $\hat{f}_{CCT}$ and $\hat{f}_R$ are the discretized distribution functions and N is the total number of samples. Applying this to the histogram of critical clearing times in Fig. 5, the probability of stability as a function of mean recloser time (with a one-cycle standard deviation) is shown in Fig. 7.

As the mean recloser time decreases, the probability that the system will be stable increases to 1.0 (100%) regardless of the standard deviation of the recloser action. This implies that the more quickly the fault is cleared, the more likely the system is to be stable. However, as the standard deviation increases from $\frac{1}{2}$ cycle to 2 cycles, the slope of the probability curve decreases. This is intuitive since as the standard deviation increases, the spread of recloser action from the mean increases, allowing greater variation. As the standard deviation approaches zero, the slope approaches infinity at $\mu = 0.233$ s and 50% probability.

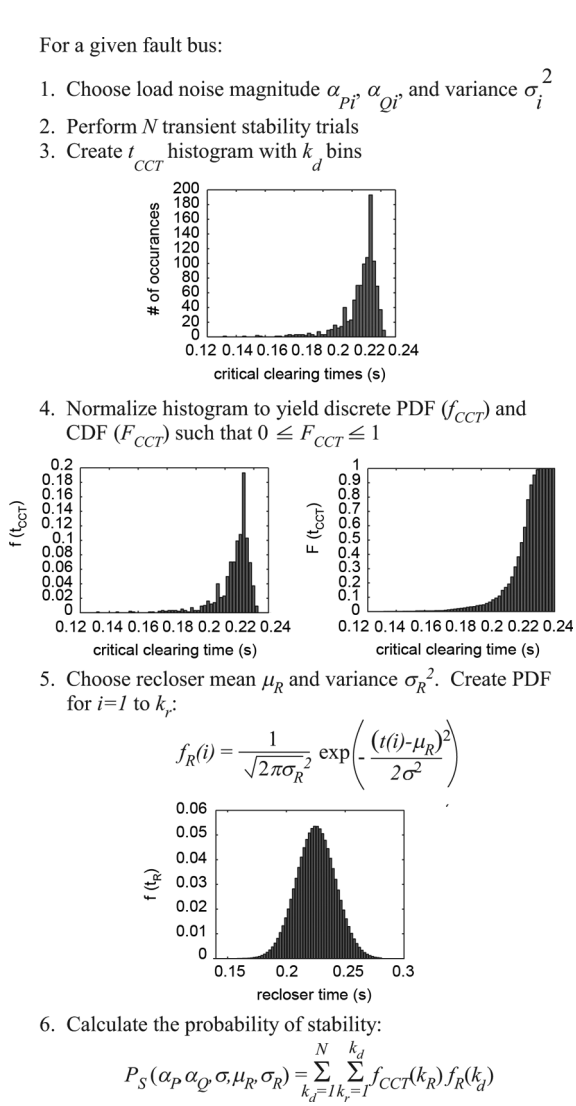

Fig. 8. Process for determining the stability of the system.

Recall that the deterministic critical clearing time is 0.233 s and is also the expected mean of the histogram of critical clearing times in Fig. 5. Therefore as the standard deviation approaches 0, the probability distribution curve of the recloser action approaches a Dirac delta and will sample only a single point at the mean (which is 0.233 s). The process for determining the probability of stability is summarized in Fig. 8.

These conclusions are predicated on the assumption that the probability of successful reclosing is 1. However, in actuality, the probability of successful reclosing can also be represented by a probability distribution function and can be incorporated as a third function into (20). Thus, as the standard deviation approaches 0, the probability of stability will approach the probability of successful reclosing.

IV. Numerical Solution of Stochastic Differential Equations

The determination of the power system energy requires the numerical solution of the SDE system. The numerical solution of SDEs is conceptually different from the numerical solution of deterministic ordinary differential equations. At the core

of the numerical solution of SDEs is the representation of the standard Wiener process over the simulation interval $[0, T_{\max}]$. The random variable $W(t)$ satisfies the three following conditions [22]:

1) $W(0) = 0$ (with probability 1)
2) For $0 \leq s < t \leq T_{\max}$, the random variable given by the increment $W(t) - W(s)$ is normally distributed with mean zero and variance $t - s$; equivalently, $W(t) - W(s) \sim \sqrt{t-s}N(0,1)$, where $N(0,1)$ denotes a normally distributed random variable with zero mean and unit variance.
3) For $0 \leq s < t < u < v \leq T_{\max}$, the increments $W(t) - W(s)$ and $W(v) - W(u)$ are independent.

A standard Wiener process $W(t)$ can be numerically approximated in distribution on any finite time interval by a scaled random walk. A stepwise continuous random walk $H_N(t)$ can be constructed by taking independent, equally probable steps of length $\pm\sqrt{\Delta t}$ at the end of each subinterval.

For the ordinary differential equation

$$\dot{x} = f(x,t), \quad x(0) = x_0 \in \mathbb{R}^n$$

the well-known Euler's method can be applied to numerically approximate the solution over $[0, T]$ [31]:

$$x_j = x_{j-1} + \Delta t f\left(x_{j-1}, t_{j-1}\right), \quad j = 1, \ldots, L \tag{22}$$

where $L\Delta t = T$ and L is a positive integer.

For the stochastic differential equation

$$dx = f(x,t)dt + g(x,t)\Sigma(t)dW(t) \quad x(0) = x_0 \in \mathbb{R}^n$$

a corresponding numerical integration method is the Euler-Maruyama (EM) method [22]:

$$x_j = x_{j-1} + \Delta t f\left(x_{j-1}, t_{j-1}\right) + g\left(x_{j-1}, t_{j-1}\right) \Sigma(t_{j-1})\left(W(\tau_j) - W(\tau_{j-1})\right) \quad j = 1, \ldots, L \tag{23}$$

where $W(\tau_j)$, $W(\tau_{j-1})$ are points on the Brownian path. The Euler-Maruyama method was selected since it is straightforward to implement. It is the simplest strong Taylor approximation, containing on the time and Wiener integrals of multiplicity one from the Ito-Taylor expansion and usually attains the order of strong convergence of 0.5. The set of points $\{t_j\}$ on which the discretized Brownian path is based must contain the points $\{\tau_j\}$ at which the EM solution is computed. If the EM is applied using a stepsize $\Delta t = R\delta t$, then

$$\left(W(\tau_j) - W(\tau_{j-1})\right) = W(jR\delta t) - W((j-1)R\delta t) \tag{24}$$

$$= \sum_{k=jR-R+1}^{jR} dW_k. \tag{25}$$

V. Application

To illustrate the application of the structure preserved stochastic energy function, the method is applied to the small power system shown in Fig. 9. This system was introduced in [30] for the study of structure preserving power systems.

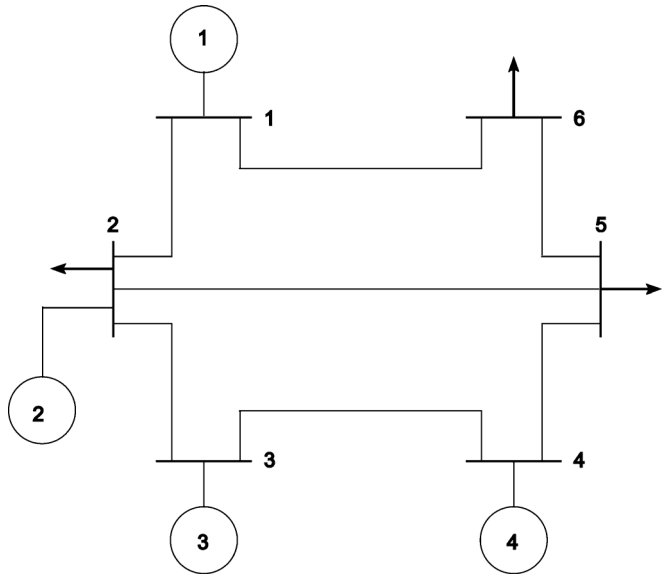

Fig. 9. Four-machine, six-bus test system.

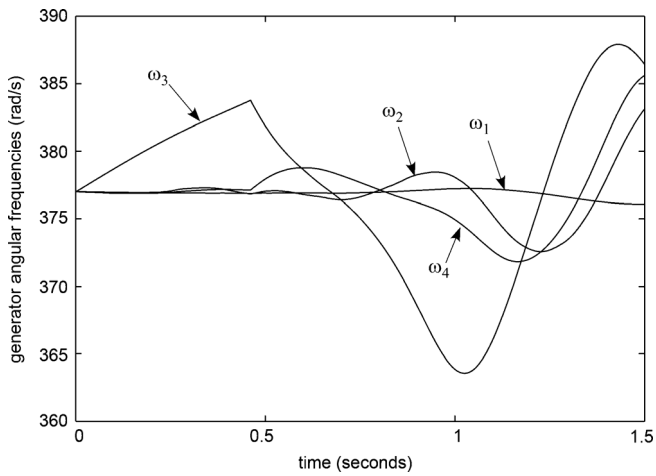

Fig. 10. Deterministic test system generator frequencies.

As a benchmark, the deterministic system is subjected to a fault on bus 3 which is cleared at 0.46 s. The resulting generator angular frequencies and bus voltages are shown in Figs. 10 and 11, respectively.

To illustrate the effect of the varying loads, ten different sets of noise with the same magnitude of variation and standard deviation are applied to the loads. The resulting noisy generator 4 frequency and bus 6 voltage are shown in Figs. 12 and 13, respectively. The mean, or expected, value of each set of responses is shown in bold. The generator frequency is much smoother than the voltage because of the impact of the integration of the noise. Generator frequency (ω) is a state variable whereas voltage is an algebraic variable and changes in load are observed instantaneously.

For the test system, the deterministic critical clearing time is determined to be 0.74 s. To further elucidate the impact of noise

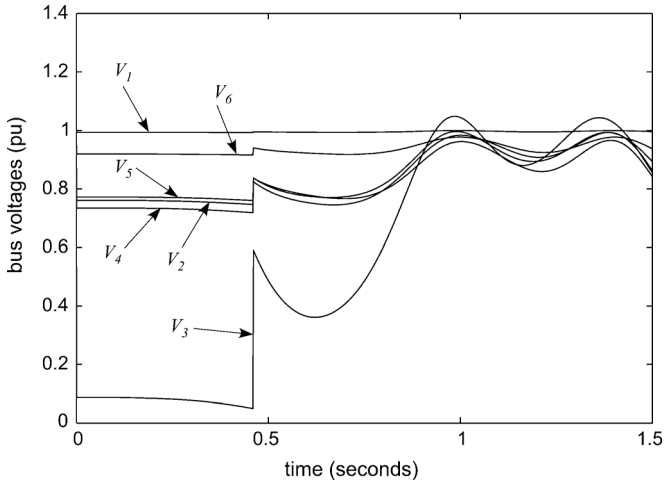

Fig. 11. Deterministic test system voltages.

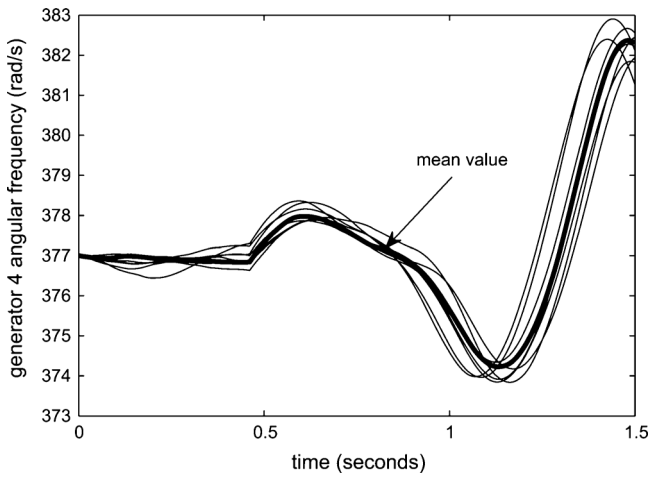

Fig. 12. Test system generator 4 frequency (ten runs).

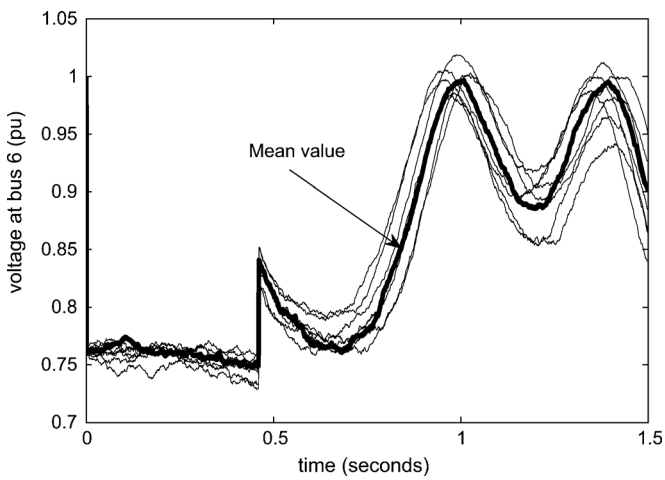

Fig. 13. Test system bus 6 voltages (ten runs).

on the critical clearing times, the critical clearing times resulting from 100 runs are plotted as a function of the inverse signal-to-noise ratio (i.e., SNR^{-1}) at a single bus (bus 5) in Fig. 14. As the level of noise in the signal decreases, the critical clearing times approach the deterministic CCT of 0.74 s. As the noise level increases, the spectrum of CCTs increase in both the larger

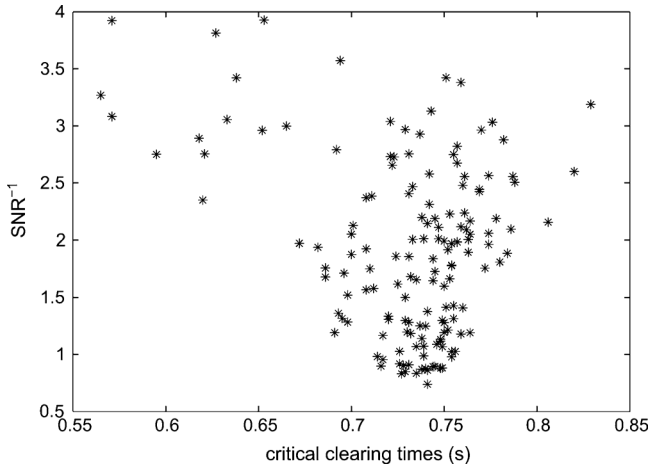

Fig. 14. Critical clearing times as a function of SNR^{-1} (100 runs).

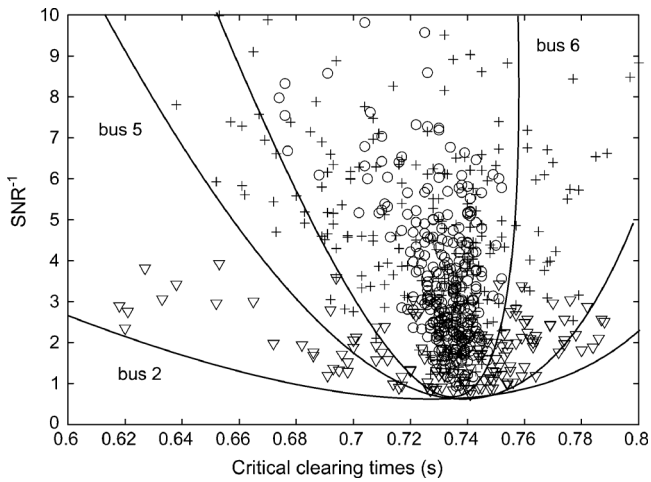

Fig. 15. Critical clearing times as a function of SNR^{-1} (100 runs); load changes at bus 2 (∇), bus 5 ($+$), and bus 6 ($\circ$).

and smaller directions, but with a greater spread towards smaller CCTs. This is an indication that as the noise level increases, the system is more likely to become unstable.

To illustrate the impact of noise at different geographic locations, equal amounts of (expected) noise are added to the different load buses and the critical clearing times are plotted. Fig. 15 shows the impact of noise added at different locations on the critical clearing time. From the figure, it can be observed that the stability of the system is most sensitive to random load variations at bus 2 (for a fault on bus 3) and least sensitive to noise levels at bus 6. It is theorized that this sensitivity is due to the proximity of the buses to the fault bus. The closer the fault is to a bus, the more sensitive the critical clearing time is to random changes in load. If information regarding penetration of wind turbines, solar panels, or other randomly varying component is available, this information can be used to scale the noise magnitudes to provide a histogram of CCTs as a function of geographical differences.

The critical clearing times shown in Fig. 15 can be converted to a histogram by enumerating the number of clearing times in a set of time intervals. This can then be used to determine the probability of stability for this system as given in Fig. 8 and the previous example.

TABLE I
SYSTEM PARAMETERS FOR THE SIX-BUS TEST SYSTEM

Transmission Line Constants			
From	To	R	X
1	2	0.05	0.2
2	3	0.10	0.5
3	4	0.20	0.80
4	5	0.10	0.30
5	6	0.20	0.40
6	1	0.10	0.15
2	5	0.20	0.50

Load data		
	Load (in MW/MVar)	
Bus	Active	Reactive
2	20.0	10.0
5	40.0	15.0
6	30.0	10.0

Generator Data			
Generator bus #	Transient reactance	Inertia constant	Generation
1	0.004	100.0	33.2
2	1.0	1.5	10.0
3	0.5	3.0	30.0
4	0.4	2.0	20.0

VI. CONCLUSIONS AND FUTURE WORK

This paper develops an approach to analyze the impact of random load and generation variations on the transient stability of a structure preserved power system. The well-known energy function method for power system transient stability is used as a basis to explore the stochastic power system stability through a stochastic Lyapunov stability analysis. Further, the method was extended numerically using the Euler-Maruyama method. It was shown that increasing the magnitude of the applied variation or changing the geographic location can have a destabilizing effect on the power system. This could potentially cause difficulties as more randomness is introduced into the power system through renewable energy sources and plug-in-hybrid vehicles.

Further work may include exploring the impact of non-Gaussian distributions on critical clearing times. An additional area of study would include modeling the stochastic behavior of generation scheduling.

APPENDIX

The parameters of the four-machine, six-bus test system are shown in Table I.

REFERENCES

[1] J. G. Vlachogiannis, "Probabilistic constrained load flow considering integration of wind power generation and electric vehicles," *IEEE Trans. Power Syst.*, vol. 24, no. 4, pp. 1808–1817, Nov. 2009.

[2] R. Billinton and P. R. S. Kuruganty, "Probabilistic assessment of transient stability in a practical multimachine system," *IEEE Trans. Power App. Syst.*, vol. PAS-100, no. 7, pp. 3634–3641, Jul. 1981.

[3] F. F. Wu and Y.-K. Tsai, "Probabilistic dynamic security assessment of power systems: Part I—Basic model," *IEEE Trans. Circuits Syst.*, vol. 30, no. 3, pp. 148–159, Mar. 1983.

[4] K. J. Timko, A. Bose, and P. M. Anderson, "Monte Carlo simulation of power system stability," *IEEE Trans. Power App. Syst.*, vol. PAS-102, no. 10, pp. 3453–3459, Oct. 1983.

[5] M. B. Do Cutto Filho, A. M. Leiti Da Silva, V. L. Arienti, and S. M. P. Ribeiro, "Probabilistic load modeling for power system expansion planning," in *Proc. IEE 3rd Int. Conf. Probabilistic Methods Applied to Electric Power Systems*, 1991, pp. 203–207.

[6] H. Mohammed and C. O. Nwankpa, "Stochastic analysis and simulation of grid-connected wind energy conversion system," *IEEE Trans. Energy Convers.*, vol. 15, no. 1, pp. 85–90, Mar. 2000.

[7] M. Meldorf, T. That, and J. Kilter, *Stochasticity of the Electrical Network Load*. Tallinn, Estonia: Estonian Academy Publishers, 2007.

[8] S. O. Faried, R. Billinton, and S. Aboreshaid, "Probabilistic evaluation of transient stability of a wind farm," *IEEE Trans. Energy Convers.*, vol. 24, no. 3, pp. 733–739, Sep. 2009.

[9] J. R. Hockenberry and B. C. Lesieutre, "Evaluation of uncertainty in dynamic simulations of power system models: The probabilistic collocation method," *IEEE Trans. Power Syst.*, vol. 19, no. 3, pp. 1483–1491, Aug. 2004.

[10] C. O. Nwankpa, S. M. Shahidehpour, and Z. Schuss, "A stochastic approach to small disturbance stability analysis," *IEEE Trans. Power Syst.*, vol. 7, no. 4, pp. 1519–1528, Nov. 1992.

[11] M. Pavella and P. G. Murthy, *Transient Stability of Power Systems: Theory and Practice*. Chichester, U.K.: Wiley, 1994.

[12] A. K. Behara, M. A. Pai, and P. W. Sauer, "Analytical approaches to determine critical clearing time in multi-machine power system," in *Proc. IEEE Conf. Decision and Control*, Dec. 1985, pp. 818–823.

[13] A. N. Michel, A. Fouad, and V. Vittal, "Power system transient stability using individual machine energy functions," *IEEE Trans. Circuits Syst.*, vol. CAS-30, no. 5, pp. 266–276, May 1983.

[14] M. K. Khedkar, G. M. Dhole, and V. G. Neve, "Transient stability analysis by transient energy function method: Closest and controlling unstable equilibrium point approach," *IE (I) Journal*, vol. 85, pp. 83–88, Sep. 2004.

[15] L. F. C. Alberto, F. H. J. R. Silva, and N. G. Bretas, "Direct methods for transient stability analysis in power systems: State of the art and future perspectives," in *Proc. IEEE Porto Power Tech Conf.*, Sep. 2001.

[16] A. R. Bergen and D. J. Hill, "A structure preserving model for power system stability analysis," *IEEE Trans. Power App. Syst.*, vol. PAS-100, no. 1, pp. 25–35, Jan. 1981.

[17] N. A. Tsolas, A. Arapostathis, and P. P. Varaiya, "A structure preserving function for power system transient stability analysis," *IEEE Trans. Circuits Syst.*, vol. CAS-32, no. 10, pp. 1041–1049, Oct. 1985.

[18] M. A. Pai, *Energy Function Analysis for Power System Stability*. Norwell, MA: Kluwer, 1989.

[19] P. Florchinger, "Lyapunov-like techniques for stochastic stability," *SIAM J. Control Optim.*, vol. 33, pp. 1151–1169, 1995.

[20] D. V. Dimarogonas and K. J. Kyriakopoulos, "Lyapunov-like stability of switched stochastic systems," in *Proc. 2004 American Control Conf.*, Boston, MA, 2004.

[21] W. Zhang, H. Zhang, and B.-S. Chen, "Generalized Lyapunov equation approach to state-dependent stochastic stabilization/detectability criterion," *IEEE Trans. Autom. Control*, vol. 53, no. 7, pp. 1630–1642, Aug. 2008.

[22] D. J. Higham, "An algorithmic introduction to numerical solution of stochastic differential equations," *SIAM Rev.*, vol. 43, no. 3, pp. 525–546, 2001.

[23] T. Burton, D. Sharpe, N. Jenkins, and E. Bossanyi, *Wind Energy Handbook*. Chichester, U.K.: Wiley, 2001.

[24] J. G. Vlachogiannis, "Probabilistic constrained load flow considering integration of wind power generation and electric vehicles," *IEEE Trans. Power Syst.*, vol. 24, no. 4, pp. 1808–1817, Nov. 2009.

[25] H.-D. Chiang, C.-C. Chu, and G. Cauley, "Direct stability analysis of electric power systems using energy functions: Theory, applications, and perspective," *Proc. IEEE*, vol. 83, no. 11, pp. 1497–1529, Nov. 1995.

[26] B. Oksendal, *Stochastic Differential Equations*. Berlin, Germany: Springer, 2007.

[27] H. Deng, M. Krstic, and R. J. Williams, "Stabilization of stochastic nonlinear systems driven by noise of unknown covariance," *IEEE Trans. Autom. Control*, vol. 46, no. 8, pp. 1237–1253, Aug. 2001.

[28] T. Weissbach and E. Welfonder, "High frequency deviations within the European power system: Origins and proposals for improvement," in *Proc. 2009 IEEE PES Power Systems Conf. Expo.*, Seattle, WA, 2009, pp. 1–6.

[29] S. O. Faried, R. Billinton, and S. Aboreshaid, "Probabilistic evaluation of transient stability of a power system incorporating wind farms," *IET Renew. Power Gen.*, vol. 4, no. 4, pp. 299–307, 2010.

[30] N. Narasimhamurthi and M. T. Musavi, "A generalized energy function for transient stability analysis of power systems," *IEEE Trans. Circuits Syst.*, vol. CAS-31, no. 7, pp. 637–645, Jul. 1984.

[31] M. L. Crow, *Computational Methods for Electric Power Systems*. Boca Raton, FL: CRC, 2009.

Theresa Odun-Ayo (S'08) received the B.Eng. degree in electrical engineering from ATBU, Bauchi, Nigeria, in 1995, the M.Eng. degree in electrical engineering from the University of Benin, Benin City, Nigeria, in 1998, and the Ph.D. degree in electrical engineering from the Missouri University of Science and Technology, Rolla, in 2011.

She worked as a Lecturer at the Nigerian Defense University for two years and as a Principal Aeronautical Engineer with the Nigerian Airspace Management Agency for five years. She is currently an Assistant Professor of electrical engineering at Missouri State University, Springfield, MO. Her research interest is in the area of power system stability and renewable energy.

Mariesa L. Crow (S'83–M'90–SM'94–F'10) received the B.S.E. degree from the University of Michigan, Ann Arbor, and the Ph.D. degree from the University of Illinois, Urbana-Champaign.

She is currently the Director of the Energy Research and Development Center and the F. Finley Distinguished Professor of Electrical Engineering at the Missouri University of Science and Technology, Rolla. Her research interests include computational methods for dynamic security assessment and the application of power electronics in bulk power systems. Prof. Crow is a Registered Professional Engineer.